Autonomic Neuroscience: Basic and Clinical 219 (2019) 33–41

Contents lists available at ScienceDirect

Autonomic Neuroscience: Basic and Clinical

journal homepage: www.elsevier.com/locate/autneu

Effects of chronic lead exposure on the sympathoexcitatory response associated with the P2X7 receptor in rat superior cervical ganglia

Gaochun Zhu[a], Bo Dai[b], Zhenying Chen[b], Liyun He[b], Jingjing Guo[c], Yu Dan[c], Shangdong Liang[c], Guilin Li[c,*]

[a] Department of Anatomy, Medical College of Nanchang University, Nanchang, PR China
[b] Department of the Fourth Clinical, Medical College of Nanchang University, Nanchang, PR China
[c] Department of Physiology, Medical College of Nanchang University, Nanchang, PR China

ARTICLE INFO

Keywords:
Lead exposure
P2X7 receptor
Satellite glial cells
Superior cervical ganglion
Sympathoexcitatory response
ERK1/2

ABSTRACT

Chronic lead exposure frequently brings about increased blood pressure and other cardiovascular diseases associated with autonomic nervous dysfunction. Purinergic signaling is involved in the development of abnormal sympathoexcitatory response due to myocardial ischemic injury. However, the potential implication of P2X7 receptor in altered sympathoexcitatory response caused by chronic lead exposure and the underlying mechanisms remain unclear. In this study, a rat model of chronic lead exposure was used to explore the changes in sympathoexcitatory response and possible involvement of P2X7 receptor in the superior cervical ganglion (SCG). Rats were divided into three groups called control, low lead and high lead groups according to daily lead exposure levels, i.e. 0, 0.5 and 2 g/L respectively. One year later, changes in P2X7 receptor expression in SCG, sympathetic nerve activity and myocardial function were measured for these rats. Our results showed that increased blood pressure and heart rate, decreased heart rate variability, enhanced cervical sympathetic nerve discharge, higher phosphorylation of ERK1/2, and up-regulated protein and mRNA levels of P2X7 expression in SCG occurred after lead exposure. In addition, double-label immunofluorescence staining of P2X7 receptor and glutamine synthetase (GS) revealed activation of the satellite glial cells of SCG by lead exposure. Moreover, knockdown of P2X7 could effectively relief the effect of lead exposure on enhanced expression of P2X7 receptor and GS. Thus our data suggest that the up-regulation of P2X7 receptor activity in satellite glial cells of SCG may contribute to the raised sympathoexcitatory response due to chronic lead exposure.

1. Introduction

Lead is widely used in making many products such as leaded gasoline, lead-based paints, and cans containing foods or alcoholic beverages (Vaziri, 2008). It is an environmentally persistent element and a major global environmental hazard (Gillis et al., 2012). Several studies have shown that lead can cause persistent and chronic impairments in humans (Grandjean, 2010; Howarth, 2004; Kossowska et al., 2013). For example, lead impaired the learning and memory functions (Nava-Ruiz et al., 2012), and caused inflammation and cardiovascular diseases (Vaziri, 2008). Lead may change the expression of genes related to the synthesis of important proteins such as connexin 43 in nerve and glial cells and affect the function of these cells (Baranowska-Bosiacka et al., 2011; Song et al., 2016).

The P2X7 receptor belongs to an adenosine triphosphate (ATP)-sensitive ionotropic P2X superfamily containing seven cloned subtypes (P2X1–P2X7) (Zhang et al., 2005). ATP is the most important energy source within all living cells. However, in addition to its metabolic function, ATP also plays a role outside the cell as a potent signaling molecule in the nervous and the immune systems (Baranowska-Bosiacka et al., 2011). High ATP concentrations (> 100 μM) can activate the P2X7 receptor which forms a pore in the membrane of cells (Cisneros-Mejorado et al., 2015; Del Puerto et al., 2015). The P2X7 receptor is found in astrocytes (Sadek et al., 2011; Zhang et al., 2005). There is evidence for ATP release from neurons in the sympathetic ganglia, apparently from preganglionic nerve terminals, and the satellite glial cell (SGC) is an obvious target for this neurotransmitter (Hanani, 2010; Messlinger and Russo, 2018). There are two distinct modes of ATP release in peripheral sensory neurons: an active process of vesicular release and a passive release following cell lysis (Cook and McCleskey, 2002; Hamilton and McMahon, 2000). ATP released from cells after tissue damage may activate P2X7 receptor expressed on SGCs

* Corresponding author at: Department of Physiology, Basic Medical College of Nanchang University, 461 Bayi Road, Nanchang, Jiangxi 330006, PR China.
E-mail address: liguilin@ncu.edu.cn (G. Li).

https://doi.org/10.1016/j.autneu.2019.03.005
Received 23 July 2018; Received in revised form 1 February 2019; Accepted 20 March 2019

in dorsal root ganglia (McGaraughty et al., 2007) or on astrocytes in brain (Baranowska-Bosiacka et al., 2011). Prolonged stimulation with a high concentration of ATP leads to a release of inflammatory mediators such as IL-1β and TNF-α, which induces cell death via the necrotic or apoptotic pathways (McGaraughty et al., 2007). P2X7 receptor is related to numerous physiological functions and pathological processes, but little is known about the potential relationship of its expression on SGCs of the superior cervical ganglia (SCG) with chronic lead exposure.

SCG plays a crucial role in the regulation of cardiac function. SCG receives efferent and afferent impulses and integrates them (Boehm and Kubista, 2002). Myocardial injury activates cardiac sympathetic afferent nerve endings, which is associated with an autonomic reflex characterized by increased blood pressure and sympathetic nerve activity (Zahner et al., 2003). On the other hand, SGCs in ganglia share many properties with astrocytes, including expression of glutamine synthetase (GS) and various neurotransmitter transporters (Hanani, 2005), and exhibit functions similar to astrocytes in the central nervous system. For example, they release proinflammatory cytokines such as IL-1β, interleukin-6 (IL-6) and monocyte chemoattractant protein-1 (MCP-1), and mediate the inflammatory response (Berta et al., 2012; Hanani, 2010). A unique feature of SGCs, which distinguishes them from astrocytes, is that they are fully surrounding individual sympathetic neurons (Hanani, 2010). Glial cells are mutually coupled by gap junctions in most regions of the nervous system (Rozental et al., 2001). A study indicates that the coupling among SGCs via gap junctions is significantly enhanced after peripheral inflammation or peripheral nerve injury (Zhang et al., 2009). In addition, during nerve injury or inflammation, SGCs demonstrate an altered phenotype similar to that seen in activated astrocytes, including increased expression of glial fibrillary acidic protein (GFAP) and glutamine synthase (GS), and enhanced synthesis of cytokines (Warwick and Hanani, 2013). One study has demonstrated that lead exposure may cause a considerable increase in GFAP expression in mouse brain regions such as the hippocampus and cortex, affecting the function of the nervous system (Kumar et al., 2014).

The nervous system is a major target of lead, which has long been regarded as an established fact. Recent evidence suggests that the effects of lead on the immune system are also related to its toxic effects on the nervous system (Chibowska et al., 2016). Chronic lead exposure can cause hypertension and cardiovascular diseases through increasing sympathetic activity (Chang et al., 2005; Pal et al., 2015; Vaziri, 2008). Activation of P2X7 receptor by extracellular ATP triggers secretion of some inflammatory substances such as IL-1β, IL-18, TNF-α and nitric oxide, and thus participates in inflammation (Alves et al., 2013). Our previous work has shown that P2X7 receptor in SCG plays a role in the sympathoexcitatory response (Kong et al., 2013; Liu et al., 2013a). Thus all available evidence indicates that glial cells are significantly implicated in the process of pathological changes in both the nervous system and heart, but the effect of lead exposure on the peripheral nerve system and underlying mechanism are currently unclear. Consequently, the present study investigated the effects of chronic lead exposure on the sympathoexcitatory response, focusing on the possible involvement of P2X7 receptor in SGCs of SCG.

2. Materials and methods

2.1. Animals and treatment

Sexually mature female and male SPF Sprague-Dawley (SD) rats (200–250 g) were obtained from the Sino-British Sippr/BK Lab Animal Ltd. (Shanghai, China). The rats were housed separately in the laboratory animal facility at room temperature (20–25 °C) in 50–60% humidity and with a 12 h light/dark cycle. The SD rats were provided with a standard chow diet of 20 g/day per rat and could access to distilled water ad libitum.

After an acclimatization period of three days, the female SD rats were randomly assigned to the different exposure groups and drank distilled water containing either 0 g/L (control), 0.5 g/L (low lead group, LLG) or 2 g/L lead acetate (high lead group, HLG) (calculate by lead) for 10 days prior to being bred with control SD male rats. The mating of rats (1 male: 2 females) was conducted overnight in standard polycarbonate cages. The mating success of the females was assessed by a vaginal plug check, and each group was fed until weaning with the above corresponding lead treatment. Ten male offspring from each group were selected and continuously given corresponding lead acetate through drinking water freely from weaning to 1 year old (Feng et al., 2016; Yu et al., 2016).

On the day of lead exposure cessation, blood pressure, ECG and other cardiac functions were measured; then after the rats were anaesthetized with 10% pentobarbital sodium (0.3 mL/100 g, i.p.), electrocardiogram (ECG) was recorded, and a whole blood sample was collected from the femoral vein and placed into an ion-free tube treated with 10% nitric acid for lead analysis. SCG were isolated for quantitative reverse transcription polymerase chain reaction (qRT-PCR), Western blotting and immunofluorescence analyses. All experiments were performed in accordance with the regulations of laboratory animal management promulgated by the Ministry of Science and Technology of the People's Republic of China [1988] No.134, which are consistent with the internationally recognized NIH guidelines for the care and use of laboratory animals.

2.2. Analysis of lead concentration in blood

The collected whole blood samples were digested with 10% HNO_3 (1 mL blood: 2.5 mL HNO_3) for 3 days in a clean room hood. Afterwards, their supernatants were used for lead analysis by inductively coupled plasma spectrometry (ICP-AES, Optima 5300 DV, PerkinElmer, Fremont, CA, USA) (Fan et al., 2010). The lead calibration standard solutions were provided by the National Research Center for Certified Reference Materials (GSB 04-1766-2004, China). The recovery rates of the samples ranged from 97.5 to 102.5%. The ICP conditions were as follows: forward RE power, 1400 W; plasma Ar flow rate, 15.0 L/min; auxiliary Ar flow rate, 0.2 L/min; nebulizer Ar flowrate, 0.85 L/min; sampling size, 1.5 mL/min; observation height, 15 mm; and integration time, 5–10 s. The metal ion content in the buffer solutions was subtracted from measurements of the samples, and the results are expressed as milligrams of metal ion per liter. To avoid possible contamination, all containers (bottles, vials, etc.) were soaked in 10% nitric acid overnight and rinsed with de-ionized water several times before use (Zhu et al., 2013).

2.3. Measurements of blood pressure and heart rate variability

Blood pressure and heart rate were determined using the indirect rat tail-cuff method (BP-98A, Softron Co., Japan). Heart rate variability (HRV) was recorded and evaluated using subcutaneous needle electrodes by the frequency-domain of electrocardiogram recordings (RM6240, ChengYi, China). Five-min ECG recording was selected for analysis. Power spectral analysis of HRV was conducted by computing the power spectrum density of the very-low frequency (VLF, 0.003–0.04 Hz), low frequency (LF, 0.04–0.15 Hz) and high frequency (HF, 0.15–0.40 Hz) components, as well as the LF/HF ratio. The power of the RR-interval variations in the whole frequency range of the spectrum, i.e. total power frequency (TP, 0–0.5 Hz), and in the ranges of VLF, LF, and HF were calculated. The LF indicates the sympathetic activity while the HF denotes the parasympathetic activity, and LF/HF ratio was calculated to estimate the sympatho-vagal balance (Berntson et al., 2008; Rajendra Acharya et al., 2006).

2.4. Measurements of sympathetic nerve activity

The postganglionic cervical sympathetic nerve discharge (SND) of

SCG was recorded and analyzed using a RM6240 biological signal analytical system (Chengdu Instrument Factory, Chengdu, China). In brief, three groups of rats were anaesthetized with pentobarbital sodium (45 mg/kg, i.p.). The left cervical sympathetic nerve was identified and immersed in warm paraffin. Silver electrodes connected to the RM6240 system for recording SND were attached to the cervical sympathetic nerve, and the reference electrode to a skin fold. The settings for the SND patterns were: recording sensitivity (25–50 μV), scanning speed (200 ms/div), power gain (200 μV), time constant (0.001 s), and frequency filtering (3 kHz). Cervical SND was integrated and quantified as μvolts × seconds (μV·s). Integrated sympathetic activity was estimated as the ratio between integrated sympathetic discharges in the lead exposure groups versus the control group. Sympathetic discharges measured after a 30-min steady state condition were considered as relevant events (Kenney et al., 2013; Lu et al., 2018).

2.5. qRT-PCR

Total messenger RNA (mRNA) was extracted from SCG using the Trizol Reagent (Invitrogen, Carlsbad, CA, USA) according to the manufacturer's instructions. After homogenization of SCG tissue, lysate was subject to the Reagent, generating an organic phase containing chloroform and an aqueous phase. RNA was precipitated by using isopropanol from the aqueous phase. Total RNA was reverse transcribed into cDNA using the RevertAid™ First Strand cDNA Synthesis Kit (Fermentas, Glen Bernie, MD, USA) according to the manufacturer's instructions. qRT-PCR was performed with SYBR-Green in the ABI 7500 PCR System. The sense and antisense primers were 5′-CTTCGGCGTGC GTTTTG-3′, 5′-AGGACAGGGTGGATCCAATG-3′ for P2X7, and 5′-CAC CCGCGAGTACAACCTTC-3′, 5′-CCCATACCCACCATCACACC-3′ for β-actin. The thermal cycling parameters were 95 °C for 30 s, followed by 40 cycles of amplification at 95 °C for 5 s and 60 °C for 30 s. The quantification of gene expression was calculated by the $2^{-\Delta\Delta Ct}$ method in comparison with respective levels of β-actin mRNA.

2.6. Knockdown of P2X7 by shRNA injection

Knockdown of P2X7 expression in SCG by injection of targeting shNRA was carried out as described previously (Carnethon et al., 2002; Guo et al., 2018). In brief, 10 μg P2X7 short hairpin RNA (P2X7 shRNA) or 10 μg scramble shRNA negative control (NC) was injected into the SCG of rats for one time (n = 10 in each group) by the Entranster™ - in vivo transfection reagents according to the manufacturer's instructions. A mixture of 10 μg P2X7 shRNA and 20 μl transfection reagent was injected into SCG for the LLG + P2X7 shRNA or HLG + P2X7 shRNA group. And for the Control + NC shRNA group, a mixture of 10 μg scramble shRNA and 20 μl transfection reagent was injected into SCG. The P2X7 shRNA and scramble shRNA were constructed by Novobio Company of Shanghai, China. After one week, SCG were isolated from various groups for determination of the expression levels of P2X7 and glutamine synthetase by Western blotting.

2.7. Western blotting

Isolated SCG were washed with ice-cold phosphate-buffered saline (PBS). The isolated tissues were homogenized by mechanical disruption in lysis buffer (50 mM Tris–Cl, pH 8.0, 150 mM NaCl, 0.1% dodecyl sodium sulfate, 1% Nonidet P-40, 0.5% sodium deoxycholate, 100 μg/mL phenylmethylsulfonyl fluoride, and 1 μg/mL aprotinin), incubated on ice for 40 min and then centrifuged at 12,000 × *g* for 10 min at 4 °C. The supernatants were collected, and protein concentrations were quantified by the Lowry method. The supernatants were diluted with loading buffer [100 mM Tris–Cl, 200 mM dithiothreitol, 4% sodium dodecylsulfate (SDS), 0.2% bromophenol blue, and 20% glycerol] and heated at 95 °C for 5 min. Equal amounts of total protein (20 μg) were loaded and separated by SDS-polyacrylamide gel (30% acrylamide, 1.5 M Tris-HCl, pH 8.8, 1.5 M Tris-HCl, pH 6.8, 10% SDS, 10% ammonium persulfate, and tetramethyl ethylene diamine) electrophoresis using running buffer containing 0.125 M Tris-Cl, 1.25 M glycine, and 10% SDS. The separated proteins were transferred onto polyvinylidene fluoride membranes (0.45 μm, Amersham Biosciences, Buckinghamshire, UK). The membranes were blocked with 5% nonfat dry milk in a solution of 25 mM Tris buffered saline pH 7.2 plus 0.1% Tween 20 (TBST) for 2 h at room temperature, followed by incubation with the primary antibodies rabbit anti-P2X7 receptor (1:1000, Sigma-Aldrich, St. Louis, MO, USA), mouse anti-glutamine synthetase (GS) (1:1500, ab64613; Abcam, Cambridge, UK), rabbit polyclonal anti-phospho-ERK1/2 (extracellular signal–regulated kinase, 1:1000, Cell Signaling Technology, Danvers, MA, USA), rabbit polyclonal anti-ERK1/2 (1:1000, Cell Signaling Technology), and mouse monoclonal anti-β-actin (1:1000, Beijing Zhongshan Biotech Co., China) overnight at 4 °C. Thereafter, membranes were incubated with the appropriate HRP-conjugated second antibody (1:2000 dilution, Beijing Zhongshan Biotech Co., China) for 1 h at room temperature. An enhanced ECL chemiluminescence development kit (Thermo Scientific, Waltham, MA, USA) and an imaging system (Bio-Rad, Hercules, CA, USA) were applied to obtain the images of protein bands. The intensity of bands was analyzed by Image-Pro Plus. The expression levels of the target proteins were calculated by normalizing to the corresponding amount of β-actin in order to avoid the interference from possible variation in loaded protein amounts between samples.

2.8. Double-label immunofluorescence staining

SCG were dissected immediately after rats were anaesthetized, washed in PBS, and fixed in 4% paraformaldehyde (PFA) for 24 h at 4 °C. The ganglia were then transferred to 20% sucrose in 4% PFA for dehydration overnight at 4 °C. Tissues were sectioned at a thickness of 12 μm with a freezing microtome, placed onto glass slides coated with poly-D-lysine, and stored at −20 °C until further processing. Co-expressions of P2X7 with glutamine synthetase (GS) or P2X7 with calcitonin gene-related peptide (CGRP) were assessed by double-label immunofluorescence. After three washes with PBS, the sections were incubated with 10% goat serum (Beijing Zhongshan Biotech Co., China) for 40 min in a moisture chamber at 37 °C to block non-specific antigens. The sections were then incubated with the mixture of either rabbit anti-P2X7 antibody (1:200, Sigma Aldrich Company, USA) plus mouse anti-GS antibody (1:200 dilution, Sigma Aldrich Company, USA) or anti-P2X7 antibody (1:200) plus mouse anti-CGRP (1:150, ab81887; Abcam, Cambridge, UK) diluted in PBS overnight at 4 °C. The sections were then rinsed and incubated with a fluorescein isothiocyanate (FITC)-conjugated goat anti-rabbit antibody (1:200, Beijing Zhongshan Biotech Co., China) and a tetraethyl rhodamine isothiocyanate (TRITC)-conjugated goat anti-mouse antibody (1:200, Beijing Zhongshan Biotech Co., China) for 1 h at room temperature in the dark. The sections were washed with PBS in the dark and mounted with an anti-fade fluorescence-mounting medium. The images were captured by fluorescence microscopy (Olympus DP72, Japan) under the same exposure, light, hue and contrast conditions. The yellow fluorescence density (co-expression level) of each image was analyzed by Image-Pro Plus software. Immunofluorescence intensity was measured in a square region of interest (100 × 100 μm) after subtracting the background which is defined as the signal measured in an area devoid of specific immunostaining. Data were collected from 5 discontinuous slices of each rat with six rats in each group.

2.9. Statistical analysis

All data were analyzed by SPSS 17.0 software. The numerical values are reported as the mean ± SE. The values of data from all tested animals (control, LLG, HLG) on sympathetic nerve discharge and immunofluorescence density were normalized to the average value of the

Table 1
Effects of lead exposure on cardiovascular parameters.

	Control (n = 10)	LLG (n = 10)	HLG (n = 10)
SBP (mmHg)	108.23 ± 5.17	116.39 ± 8.56*	124.26 ± 9.46**,#
DBP (mmHg)	83.88 ± 5.95	84.03 ± 6.58	87.89 ± 9.85*,#
Heart rate (bpm)	367.76 ± 14.90	389.72 ± 15.21*	419.15 ± 18.52**,##
TP (ms^2)	587.52 ± 112.23	468.79 ± 117.05**	427.47 ± 100.17**,#
VLF (ms^2)	305.96 ± 74.35	253.38 ± 87.29*	198.82 ± 46.38**,#
LF (ms^2)	73.57 ± 17.95	64.48 ± 19.56*	59.98 ± 19.67**
HF (ms^2)	153.52 ± 47.36	110.16 ± 48.56*	78.37 ± 25.58**,#
LF/HF	0.49 ± 0.08	0.59 ± 0.09*	0.79 ± 0.11**,##

The vales are mean ± SE.
* $p < 0.05$.
** $p < 0.01$ vs the control group.
# $p < 0.05$.
$p < 0.01$ vs the LLG group.

control group, as performed previously (Guo et al., 2018; Kenney et al., 2013; Lu et al., 2018). Statistical significance was determined by one-way analysis of variance (ANOVA) followed by the Fisher post hoc test for multiple comparisons. A value of $p < 0.05$ was considered statistically significant.

3. Results

3.1. Effects of lead exposure on blood pressure and heart rate variability

After lead exposure for 1 year, the systolic blood pressure (SBP) in LLG group and diastolic blood pressure (DBP) in HLG group were higher than those in the control group ($p < 0.05$); more significant increase of SBP was observed in HLG group compared with the control group ($p < 0.01$) (Table 1). In addition, both the SBP and DBP were significantly higher in the HLG than in the LLG ($p < 0.05$). There was no significant difference in the DBP between the control group and LLG. These results suggested that SBP was increasing upon exposure to the increased lead concentrations. Moreover, the heart rate (HR) in lead exposure rats was faster than that in the control group, an effect also dependent on lead dosages (Table 1).

A frequency-domain analysis showed that TP, VLF, LF and HF were decreased in both the LLG and HLG compared with the control group (Table 1), suggesting that both the sympathetic and parasympathetic activities were reduced in the LLG and HLG rats. However, compared with the control group, the LF/HF ratio was significantly increased in the LLG ($p < 0.05$) and HLG ($p < 0.01$), pointing to the uneven damage that reduced the parasympathetic activity more than the sympathetic activity. The extent of decrease in TP, VLF, LF and HF was greater in the HLG rats in comparison to those in the LLG rats. HLG rats also exhibited higher LF/HF ratio than the LLG rats ($p < 0.01$), suggesting that the imbalance between the sympathetic tone and parasympathetic tone was larger in the HLG than the LLG, and in other word, the sympathetic nerve was relatively more excited in the former rats (Table 1).

3.2. Effect of lead exposure on sympathetic nerve activity

The postganglionic cervical SND of SCG in the LLG and HLG was significantly enhanced compared with that in the control group ($p < 0.01$, Fig. 1), and the increase occurred in a lead dose-dependent manner. Thus the increased sympathetic nerve activity in the lead exposure rats is in line with the raised excitability in cardiac sympathetic nerve.

3.3. Impact of chronic lead intake on lead concentration in blood

The lead concentration in blood in lead exposure groups was higher than that in the control group ($p < 0.01$, Table 2). In addition, HLG rats displayed a significantly higher lead concentration in blood than LLG rats ($p < 0.01$).

3.4. Effect of lead exposure on P2X7 expression at mRNA and protein levels in SCG

The total RNA isolated from SCG of rats exposed to lead for 1 year was subject to qRT-PCR analysis to quantify the mRNA levels of P2X7 receptor. The transcript levels of P2X7 receptor in both the LLG and HLG were remarkably increased compared with that in the control group ($p < 0.01$, Fig. 2A). Furthermore, expression of P2X7 at the mRNA level in the HLG was significantly higher than that in the LLG ($p < 0.01$).

Expression of P2X7 receptor at the protein level was further analyzed by Western blotting. By quantification of the band intensity, the stain values (integrated optical density, IOD) of P2X7 receptor protein (normalized to individual β-actin internal control) in the LLG and HLG were significantly higher than that in the control group (Fig. 2B, C). In addition, P2X7 protein content in the HLG was also higher than that in the LLG ($p < 0.01$).

3.5. Effect of lead exposure on double-label immunofluorescence staining of P2X7 with GS or CGRP in SCG

The main glial cell type in most sympathetic ganglion tissues is the SGC. SGCs usually form envelopes around individual neurons. The presence of GS is the typical feature of SGCs. An increase of GS in SCG indicates activation of SGCs upon nervous injury (Zou et al., 2012). The co-expression of GS and P2X7 was determined by double-label immunofluorescence staining. Co-localization of P2X7 receptor and GS was found mainly in the SGCs of SCG in all groups of rats (Fig. 3A). The staining of GS and P2X7 in the lead-exposed groups was more intense than that in the control group ($p < 0.01$; Fig. 3B). In addition, double-label immunofluorescence staining was also performed for P2X7 and CGRP; the latter is expressed in the neurons of SCG (Zaidi and Matthews, 2013). The results confirmed that CGRP was expressed in neurons whereas P2X7 was surrounded rather than co-localized with the neuron (Fig. 3D), indicating that P2X7 receptor was expressed in SGCs rather than neurons. Moreover, Western blotting also revealed that the expression of GS in SCG at the protein level in the LLG and HLG was higher than that in the control group ($p < 0.01$; Fig. 3C), under similar experimental conditions where the same pattern of changes were seen for both GS and P2X7 (see Fig. 2B). These data indicated that P2X7 receptor was expressed in SGCs of SCG and furthermore, up-regulated co-expression of GS and P2X7 receptor occurred in SGCs due to lead exposure, likely resulting from activation of SGCs by ATP stimulation of increased P2X7 receptors.

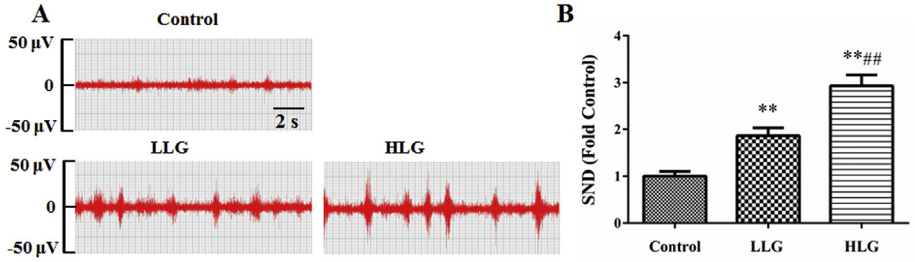

Fig. 1. Effects of lead exposure on cervical sympathetic nerve activity. (A) Representative recordings of the postganglionic cervical sympathetic nerve discharge (SND) of SCG. (B) Integrated cervical SND in all groups. Values are mean ± SE (n = 10). **$p < 0.01$ vs Ctrl; ##$p < 0.01$ vs the LLG group.

Table 2
The lead concentration in blood of rats.

	Control (n = 10)	LLG (n = 10)	HLG (n = 10)
Lead concentration (mg/L)	0	0.27 ± 0.02**	0.54 ± 0.05**,##

The values are mean ± SE.
** $p < 0.01$ vs control group.
$p < 0.01$ vs LLG group.

3.6. Effect of P2X7 shRNA on the expression of P2X7 and GS in SCG

To determine whether P2X7 regulated activation of SGCs due to lead exposure, the expression levels of P2X7 and GS in SCG were detected by Western blotting after knockdown by shRNA injection (Fig. 4A). The IOD ratio of P2X7 to β-actin was significantly higher in the LLG and HLG groups than the control group ($p < 0.01$, Fig. 4B), as similarly observed above. However, injection of P2X7 shRNA remarkably counteracted the upregulated expression of P2X7 in both the LLG and HLG groups ($p < 0.01$). In addition, exposure to lead also significantly increased the IOD ratio of GS to β-actin in a dose-dependent manner ($p < 0.01$, Fig. 4C). Likewise, the upregulated expression levels of GS in the LLG and HLG groups were also effectively inhibited by the treatment of P2X7 shRNA ($p < 0.01$). Treatment with scramble shRNA did not alter the expression of P2X7 and GS in control group ($p > 0.05$).

3.7. Effect of lead exposure on phosphorylation of ERK1/2 in SCG

The expression levels of ERK1/2 and its active p-ERK1/2 were detected by Western blotting (Fig. 5A). The IOD ratio of ERK1/2 to β-actin was not significantly different among the three groups ($F_{(2,6)} = 2.98$, $p = 0.12$, Fig. 5B). However, the phosphorylation levels of ERK1/2 (IOD ratio of p-ERK1/2 to ERK1/2) in the LLG and HLG were remarkably higher than that in the control group ($p < 0.01$, Fig. 5C). Furthermore, such effect on the IOD ratio of p-ERK1/2 to ERK1/2 was larger in the HLG than the LLG ($p < 0.05$).

4. Discussion

Lead exposure produces sustained and chronic harm to human health (Gillis et al., 2012). Data from animal experiments and population investigations prove that lead exposure results in elevated blood pressure and cardiovascular injury (Tsao et al., 2000), but the underlying mechanisms remain to be fully elucidated. In order to explore the effect of long-term lead exposure on sympathoexcitatory response, a one-year treatment was chosen for this study, in view of the fact that chronic lead exposure to human being occurs in most real environment. The effects of lead exposure for 1 year on neurotoxicity in rats have also been reported (Feng et al., 2016). Of course, it cannot be ruled out that shorter lead exposure may also affect nervous and cardiovascular

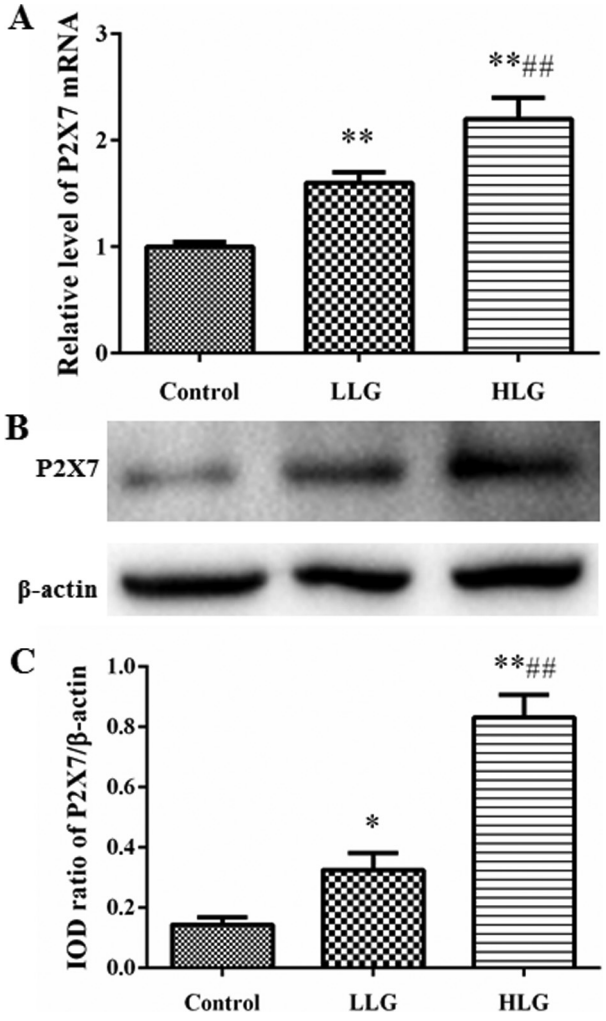

Fig. 2. Lead exposure increased P2X7 expression in SCG of rats. (A) The mRNA level of P2X7 was quantified by qRT-PCR using β-actin as the internal control. Results were expressed as mean ± SE of the fold changes from three independent experiments. (B) Detection of P2X7 protein by Western blotting in SCG of lead-exposed rats. (C) The bar histograms show the IOD ratio of P2X7 protein contents relative to β-actin in each group. Values are mean ± SE from three independent experiments. *$p < 0.05$, **$p < 0.01$ vs the control group; ## $p < 0.01$ vs the LLG group.

functions. Our results showed that SBP, DBP and HR in rats exposure to lead for 1 year were increased, and the effects were dose-dependent on the lead concentration. This implied that lead exposure could raise sympathetic nerve activity. Our data also indicated that lead exposure decreased the HRV, including both the LF and HF, but increased the LF/HF ratio. Reduced HRV can increase the risk for developing human atherosclerosis, coronary heart disease and other cardiovascular

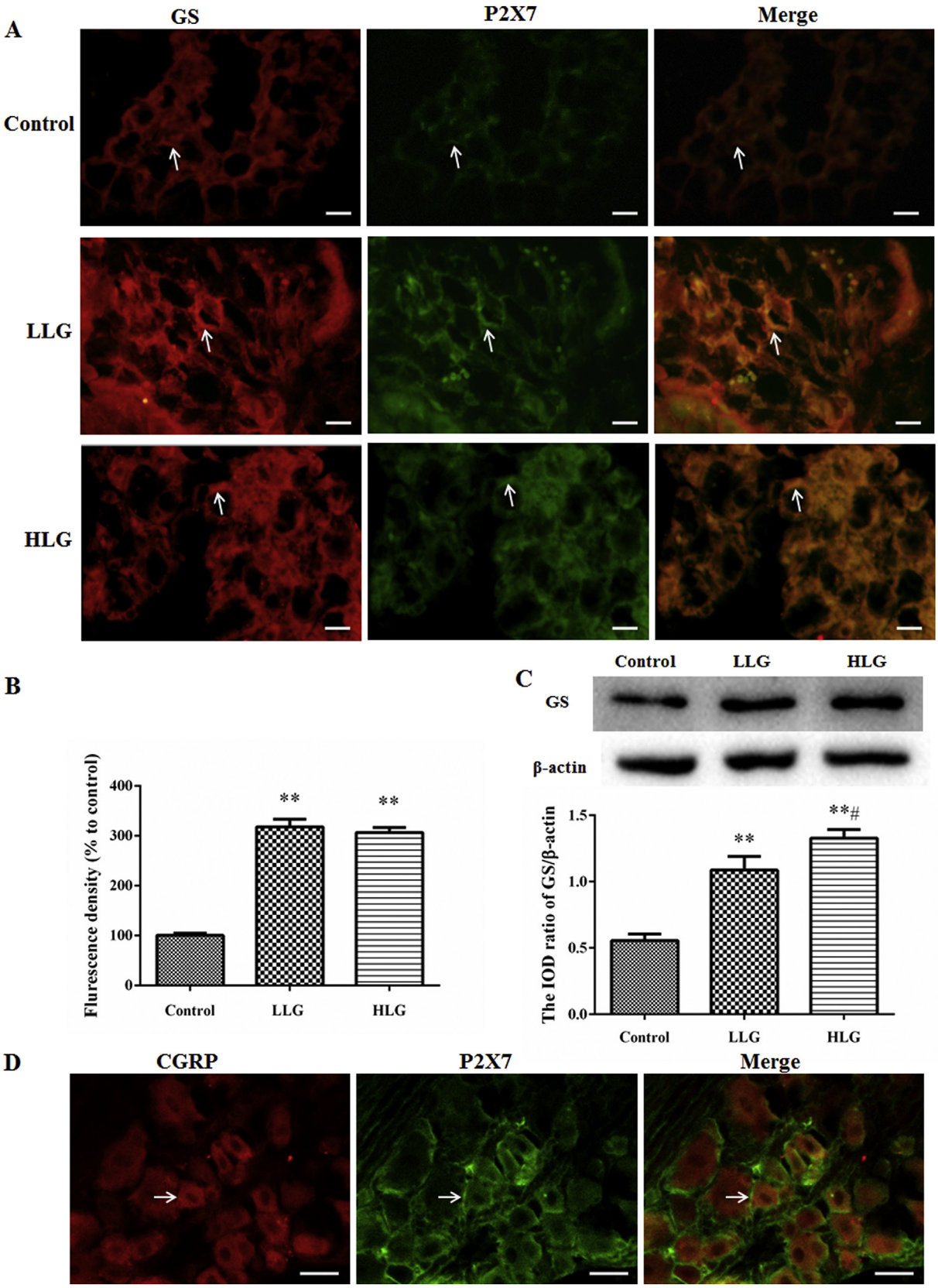

(caption on next page)

diseases, and also raise the mortality of cardiovascular diseases (Carnethon et al., 2002). Neurons in SCG receive efferent and afferent impulses and integrate a variety of information, playing an important role in the regulation of cardiac function (Armour, 1999). Our work revealed that both the sympathetic and parasympathetic activity were impaired after lead exposure, but with parasympathetic tone more

Fig. 3. Double-label immunofluorescence staining and the expression of GS protein in SCG. (A) GS and P2X7 receptor were co-expressed in SCG. The red color (TRITC) indicates GS staining; the green color (FITC) indicates P2X7 staining; and the merge image represents double-staining of P2X7 and GS. Arrows indicate the immuno-stained SGCs. Images are the representative from 10 rats in each group. Scale bar: 50 μm (B) Quantification of P2X7 receptor and GS co-immunostaining (yellow) fluorescence, with the fluorescence density in control group as 100% (n = 6 in each group). $^{**}p < 0.01$ vs Ctrl. (C) The bar histograms show the IOD ratio of GS protein level relative to β-actin in each group, as assessed by Western blotting. Values are mean ± SE from three independent experiments. $^{**}\ p < 0.01$ vs Ctrl; $^{\#}\ p < 0.05$ vs LLG. (D) The double-label immunofluorescence staining of P2X7 and CGRP in SCG. The green signal represents P2X7 staining with FITC, and the red signal indicates CGRP staining with TRITC. The merged image represents the double staining of P2X7 and CGRP. Scale bar, 50 μm. (For interpretation of the references to color in this figure legend, the reader is referred to the web version of this article.)

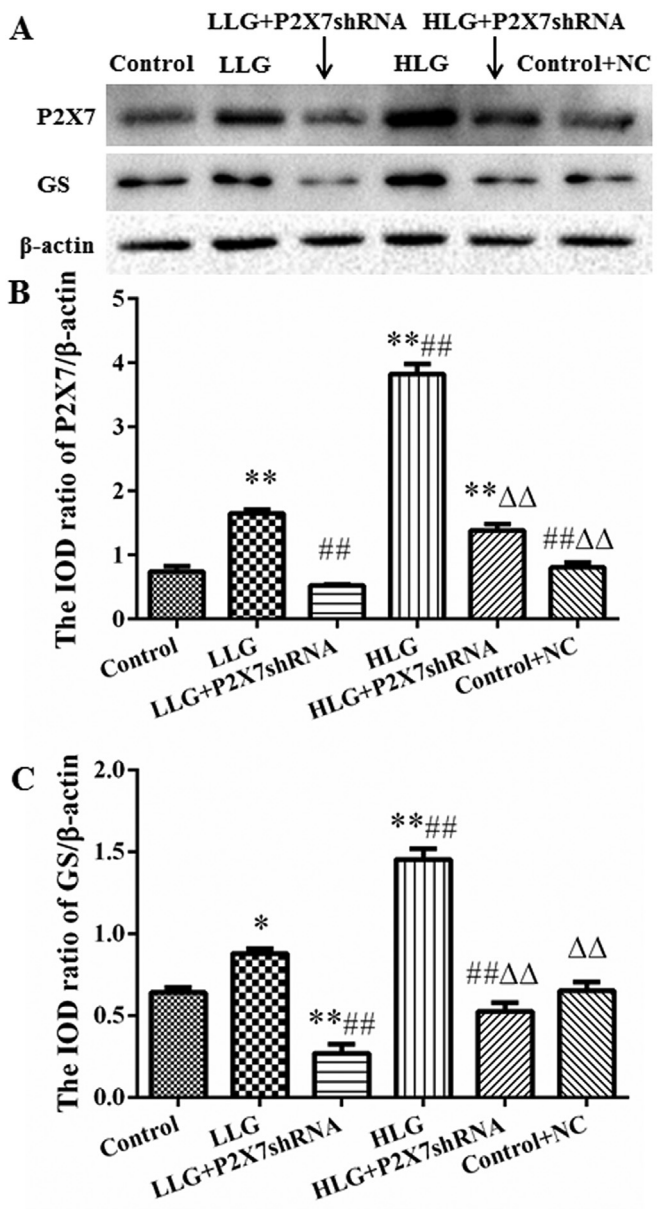

Fig. 4. P2X7 shRNA counteracted the enhanced expression of P2X7 and GS in SCG due to lead exposure. (A) The expression levels of P2X7 and GS in SCG was detected by Western blotting. (B) The bar histogram shows the IOD ratio of P2X7 protein level relative to β-actin in each group. (C) The bar histogram shows the IOD ratio of GS protein level relative to β-actin in each group. Values are mean ± SE from three independent experiments. $^{*}\ p < 0.05$ and $^{**}\ p < 0.01$ vs the control group; $^{\#\#}\ p < 0.01$ vs the LLG group; $^{\Delta\Delta}\ p < 0.01$ vs the HLG group.

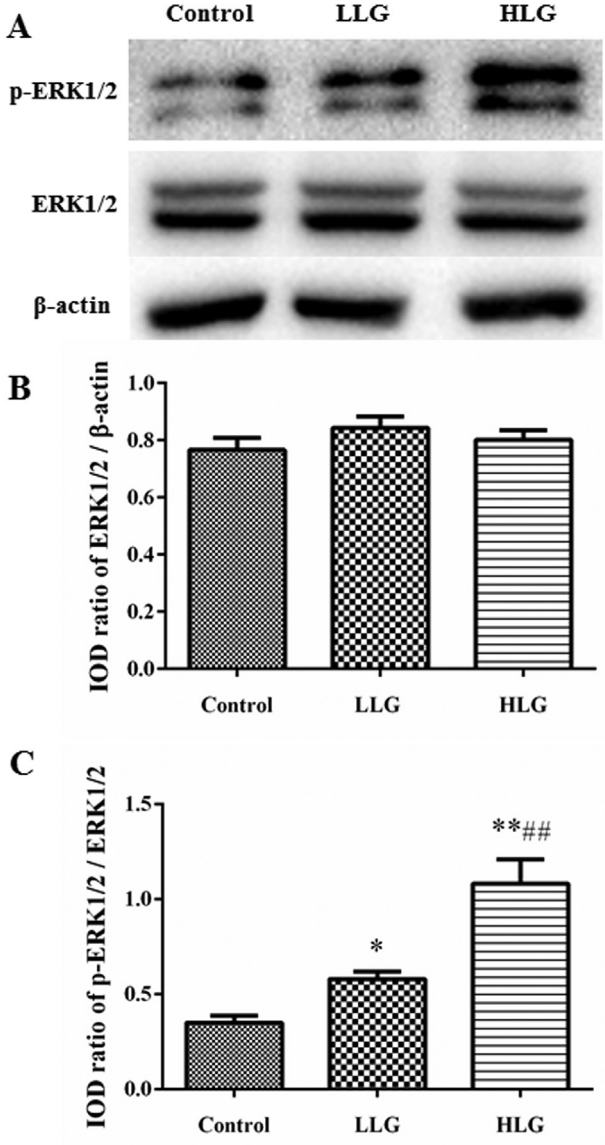

Fig. 5. Lead exposure increased phosphorylation of ERK1/2 in SCG. (A) The expression of ERK1/2 and p-ERK1/2 was detected by Western blotting. (B) The bar histograms show the IOD ratio of ERK1/2 protein level relative to β-actin in each group. (C) The bar histograms showed the IOD ratio of p-ERK1/2 to ERK1/2 in each group. The values are mean ± SE from three independent experiments. $^{**}\ p < 0.01$ vs control group; $^{\#}\ p < 0.05$ vs the LLG group.

severely reduced. Therefore, an imbalance between the sympathetic and parasympathetic nerve ensued, resulting in a relatively more excited sympathetic system eventually. The cervical sympathetic ganglion neurons participate in regulating the function of heart and blood vessels (Tu et al., 2013). In our study, lead exposure also enhanced the cervical SND, confirming the increased excitability of the cardiac sympathetic nerve, which would result in the up-regulation of the blood pressure and heart rate.

Lead exposure can cause neurotoxicity including nerve injury (Liu et al., 2013b; Zhang et al., 2014), and some studies have shown that ATP is released from injured tissues (Burnstock, 2016; Davalos et al., 2005). ATP is present in the millimolar range in cytosol, while

extracellular ATP may activate P2X receptors at the micromolar level (Cook and McCleskey, 2002). Extracellular ATP evokes various physiological responses in different tissues via P2 receptors which are classified into ligand-gated ion channel P2X receptors and metabotropic G protein-coupled P2Y receptors (Burnstock, 2004). The P2X7 receptor is an ATP-sensitive ligand-gated nonselective cation channel (Zhang et al., 2005). In central nervous system, P2X7 receptor is expressed in both glial cells such as microglial cells, Schwann cells and astrocytes (Fields and Burnstock, 2006; Sim et al., 2004; Vaziri and Gonick, 2008) and in neurons of different regions including cerebellum, hippocampus, cerebral cortex, medulla oblongata and spinal cord (Sanchez-Nogueiro et al., 2014; Sim et al., 2004). By contrast, in the peripheral ganglia of rats, P2X7 receptor is also expressed in the glial cells of SCG (Kong et al., 2013; Zhang et al., 2005), but apparently not in the neurons since our current double-label immunofluorescence studies revealed that P2X7 receptor was co-expressed with the maker of glial cells (GS) rather than with the marker of neurons (CGRP). This suggested that P2X7 receptor was mainly expressed in the SGCs of SCG. The nervous system is the main target of lead exposure and the developing brain is especially sensitive to lead (Li et al., 2015). Neurons communicate each other and also with glial cells through release of transmitters such as ATP. Chronic lead exposure frequently hurts the neurons (Baranowska-Bosiacka et al., 2011). The injured sympathetic ganglion neurons and preganglionic fibers evoke increased release of ATP (Gu et al., 2010). The extra extracellular ATP would bind to the P2X7 receptor expressed on SGCs of SCG and activate them. Consequently, the activated glial cells may release more pro-inflammatory factors and ATP, which aggravates neuronal impairments (Hanani, 2010; Verkhratsky et al., 2011).

Lead exposure may alter the expression of important genes in nervous cells and glial cells, affecting the functions of these cells. Our results displayed that the expression of P2X7 receptor at both mRNA and protein levels in SCG was up-regulated after lead exposure. Double-labeling immunofluorescence staining showed that co-expression of P2X7 receptor and GS in SGCs was up-regulated. Since GS was considered as the indicator of glial cell activation, the increased expression of GS in SGCs due to lead exposure suggested that their activation might be mediated by raised activity of P2X7 receptor subsequent of stronger ATP stimulation. This notion was supported by the results from the experiments using shRNA injection into SCG, where knockdown of P2X7 receptor could effectively counteracted the enhanced expression of GS due to lead exposure. The available evidence from our previous and other studies strongly suggests a close connection of P2X7 activity of SCG to sympathoexcitatory response for cardiovascular regulation (Kong et al., 2013; Liu et al., 2013a; Tu et al., 2013; Zaidi and Matthews, 2013), which may contribute to the abnormal cardiovascular parameters such as higher SBP, DBP and HR in rats after lead exposure. In addition, the activated SGCs may release more proinflammatory cytokines (Berta et al., 2012; Hanani, 2010; Lei et al., 2016; Liang et al., 2010), promoting sympathetic nerve activity (Fan et al., 2018).

ERK1/2 is a key player in the signaling pathways mediated by mitogen-activated serine/threonine protein kinases and may direct cellular responses to a diverse array of stimuli such as heat shock and proinflammatory cytokines. Activation of P2X7 receptor involves the initiation of ERK1/2-mediated signal transduction (Barbieri et al., 2008; Okumura et al., 2008; Sperlagh et al., 2006). The P2X7 agonist, BzATP, induces ERK1/2 phosphorylation, whereas the P2X7 antagonist, BBG, inhibits the BzATP-induced ERK activation (Okumura et al., 2008; Sperlagh et al., 2006). Our results showed that the phosphorylation levels of ERK1/2 (IOD ratios of p-ERK1/2 to ERK1/2) in the lead exposure groups were remarkably higher than that in the control group, suggesting that the ERK1/2-mediated signaling pathway might participate in the raised sympathoexcitatory response secondary to the elevated P2X7 receptor activity in chronic lead-exposed rats.

5. Summary

Chronic lead exposure caused imbalanced injury to the sympathetic and parasympathetic nerve functions especially the latter in a dose-dependent manner, resulting in the enhanced sympathoexcitatory response in cardiovascular system. The underlying molecular mechanism for these abnormalities was probably related to the up-regulated expression of P2X7 receptor, activation of SGC, and stimulation of ERK1/2-mediated signaling pathway in SCG.

Declaration of interest

The authors declare that there is no conflict of interest.

Acknowledgment

This study was supported by grants from the National Natural Science Foundation of China (31860273, 81860217, 81560219, 81360436 and 81200853), a grant from the Young Scientist Training Project of Jiangxi Province, China (20153BCB23030), and grant from the Natural Science Foundation of Jiangxi Province, China (20171BAB205025).

References

Alves, L.A., Bezerra, R.J., Faria, R.X., Ferreira, L.G., da Silva Frutuoso, V., 2013. Physiological roles and potential therapeutic applications of the P2X7 receptor in inflammation and pain. Molecules 18, 10953–10972.
Armour, J.A., 1999. Myocardial ischaemia and the cardiac nervous system. Cardiovasc. Res. 41, 41–54.
Baranowska-Bosiacka, I., Dabrowska-Bouta, B., Struzynska, L., 2011. Regional changes in purines and selected purinergic receptors in immature rat brain exposed to lead. Toxicology 279, 100–107.
Barbieri, R., Alloisio, S., Ferroni, S., Nobile, M., 2008. Differential crosstalk between P2X7 and arachidonic acid in activation of mitogen-activated protein kinases. Neurochem. Int. 53, 255–262.
Berntson, G.G., Norman, G.J., Hawkley, L.C., Cacioppo, J.T., 2008. Cardiac autonomic balance versus cardiac regulatory capacity. Psychophysiology 45, 643–652.
Berta, T., Liu, T., Liu, Y.C., Xu, Z.Z., Ji, R.R., 2012. Acute morphine activates satellite glial cells and up-regulates IL-1beta in dorsal root ganglia in mice via matrix metalloprotease-9. Mol. Pain 8, 18.
Boehm, S., Kubista, H., 2002. Fine tuning of sympathetic transmitter release via ionotropic and metabotropic presynaptic receptors. Pharmacol. Rev. 54, 43–99.
Burnstock, G., 2004. Introduction: P2 receptors. Curr. Top. Med. Chem. 4, 793–803.
Burnstock, G., 2016. P2X ion channel receptors and inflammation. Purinergic Signalling 12, 59–67.
Carnethon, M.R., Liao, D., Evans, G.W., Cascio, W.E., Chambless, L.E., Rosamond, W.D., Heiss, G., 2002. Does the cardiac autonomic response to postural change predict incident coronary heart disease and mortality? The Atherosclerosis Risk in Communities Study. Am. J. Epidemiol. 155, 48–56.
Chang, H.-R., Tsao, D.-A., Yu, H.-S., Ho, C.-K., 2005. The change of β-adrenergic system after cessation of lead exposure. Toxicology 207, 73–80.
Chibowska, K., Baranowska-Bosiacka, I., Falkowska, A., Gutowska, I., Goschorska, M., Chlubek, D., 2016. Effect of lead (Pb) on inflammatory processes in the brain. Int. J. Mol. Sci. 17.
Cisneros-Mejorado, A., Perez-Samartin, A., Gottlieb, M., Matute, C., 2015. ATP signaling in brain: release, excitotoxicity and potential therapeutic targets. Cell. Mol. Neurobiol. 35, 1–6.
Cook, S.P., McCleskey, E.W., 2002. Cell damage excites nociceptors through release of cytosolic ATP. Pain 95, 41–47.
Davalos, D., Grutzendler, J., Yang, G., Kim, J.V., Zuo, Y., Jung, S., Littman, D.R., Dustin, M.L., Gan, W.B., 2005. ATP mediates rapid microglial response to local brain injury in vivo. Nat. Neurosci. 8, 752–758.
Del Puerto, A., Fronzaroli-Molinieres, L., Perez-Alvarez, M.J., Giraud, P., Carlier, E., Wandosell, F., Debanne, D., Garrido, J.J., 2015. ATP-P2X7 receptor modulates axon initial segment composition and function in physiological conditions and brain injury. Cereb. Cortex 25, 2282–2294.
Fan, G., Feng, C., Wu, F., Ye, W., Lin, F., Wang, C., Yan, J., Zhu, G., Xiao, Y., Bi, Y., 2010. Methionine choline reverses lead-induced cognitive and N-methyl-d-aspartate receptor subunit 1 deficits. Toxicology 272, 23–31.
Fan, Y., Jiang, E., Hahka, T., Chen, Q.H., Yan, J., Shan, Z., 2018. Orexin A increases sympathetic nerve activity through promoting expression of proinflammatory cytokines in Sprague Dawley rats. Acta Physiol. 222.
Feng, C., Gu, J., Zhou, F., Li, J., Zhu, G., Guan, L., Liu, H., Du, G., Feng, J., Liu, D., Zhang, S., Fan, G., 2016. The effect of lead exposure on expression of SIRT1 in the rat hippocampus. Environ. Toxicol. Pharmacol. 44, 84–92.
Fields, R.D., Burnstock, G., 2006. Purinergic signalling in neuron-glia interactions. Nat. Rev. Neurosci. 7, 423–436.

Gillis, B.S., Arbieva, Z., Gavin, I.M., 2012. Analysis of lead toxicity in human cells. BMC Genomics 13, 344.
Grandjean, P., 2010. Even low-dose lead exposure is hazardous. Lancet 376, 855–856.
Gu, Y., Chen, Y., Zhang, X., Li, G.W., Wang, C., Huang, L.Y., 2010. Neuronal soma-satellite glial cell interactions in sensory ganglia and the participation of purinergic receptors. Neuron Glia Biol. 6, 53–62.
Guo, J., Sheng, X., Dan, Y., Xu, Y., Zhang, Y., Ji, H., Wang, J., Xu, Z., Che, H., Li, G., Liang, S., Li, G., 2018. Involvement of P2Y12 receptor of stellate ganglion in diabetic cardiovascular autonomic neuropathy. Purinergic Signalling 14, 345–357.
Hamilton, S.G., McMahon, S.B., 2000. ATP as a peripheral mediator of pain. J. Auton. Nerv. Syst. 81, 187–194.
Hanani, M., 2005. Satellite glial cells in sensory ganglia: from form to function. Brain Res. Brain Res. Rev. 48, 457–476.
Hanani, M., 2010. Satellite glial cells in sympathetic and parasympathetic ganglia: in search of function. Brain Res. Rev. 64, 304–327.
Howarth, D., 2004. Lead exposure—implications for general practice. Aust. Fam. Physician 41, 311.
Kenney, M.J., Ganta, C.K., Fels, R.J., 2013. Disinhibition of RVLM neural circuits and regulation of sympathetic nerve discharge at peak hyperthermia. J. Appl. Physiol. 115, 1297–1303.
Kong, F., Liu, S., Xu, C., Liu, J., Li, G., Li, G., Gao, Y., Lin, H., Tu, G., Peng, H., Qiu, S., Fan, B., Zhu, Q., Yu, S., Zheng, C., Liang, S., 2013. Electrophysiological studies of upregulated P2X7 receptors in rat superior cervical ganglia after myocardial ischemic injury. Neurochem. Int. 63, 230–237.
Kossowska, B., Dudka, I., Gancarz, R., Antonowicz-Juchniewicz, J., 2013. Application of classic epidemiological studies and proteomics in research of occupational and environmental exposure to lead, cadmium and arsenic. Int. J. Hyg. Environ. Health 216, 1–7.
Kumar, P., Singh, R., Nazmi, A., Lakhanpal, D., Kataria, H., Kaur, G., 2014. Glioprotective effects of Ashwagandha leaf extract against lead induced toxicity. Biomed. Res. Int. 2014, 182029.
Lei, Y., Sun, Y., Lu, C., Ma, Z., Gu, X., 2016. Activated glia increased the level of proinflammatory cytokines in a resiniferatoxin-induced neuropathic pain rat model. Reg. Anesth. Pain Med. 41, 744–749.
Li, N., Zhang, P., Qiao, M., Shao, J., Li, H., Xie, W., 2015. The effects of early life lead exposure on the expression of P2X7 receptor and synaptophysin in the hippocampus of mouse pups. J. Trace Elem. Med. Biol. 30, 124–128.
Liang, L., Wang, Z., Lu, N., Yang, J., Zhang, Y., Zhao, Z., 2010. Involvement of nerve injury and activation of peripheral glial cells in tetanic sciatic stimulation-induced persistent pain in rats. J. Neurosci. Res. 88, 2899–2910.
Liu, J., Li, G., Peng, H., Tu, G., Kong, F., Liu, S., Gao, Y., Xu, H., Qiu, S., Fan, B., Zhu, Q., Yu, S., Zheng, C., Wu, B., Peng, L., Song, M., Wu, Q., Li, G., Liang, S., 2013a. Sensory-sympathetic coupling in superior cervical ganglia after myocardial ischemic injury facilitates sympathoexcitatory action via P2X7 receptor. Purinergic Signalling 9, 463–479.
Liu, K.S., Hao, J.H., Zeng, Y., Dai, F.C., Gu, P.Q., 2013b. Neurotoxicity and biomarkers of lead exposure: a review. Chin. Med. Sci. J. 28, 178–188.
Lu, Y., Wu, Q., Liu, L.Z., Yu, X.J., Liu, J.J., Li, M.X., Zang, W.J., 2018. Pyridostigmine protects against cardiomyopathy associated with adipose tissue browning and improvement of vagal activity in high-fat diet rats. Biochim. Biophys. Acta 1864, 1037–1050.
McGaraughty, S., Chu, K.L., Namovic, M.T., Donnelly-Roberts, D.L., Harris, R.R., Zhang, X.F., Shieh, C.C., Wismer, C.T., Zhu, C.Z., Gauvin, D.M., Fabiyi, A.C., Honore, P., Gregg, R.J., Kort, M.E., Nelson, D.W., Carroll, W.A., Marsh, K., Faltynek, C.R., Jarvis, M.F., 2007. P2X7-related modulation of pathological nociception in rats. Neuroscience 146, 1817–1828.
Messlinger, K., Russo, A.F., 2018. Current understanding of trigeminal ganglion structure and function in headache. Cephalalgia (Epub ahead of print).
Nava-Ruiz, C., Méndez-Armenta, M., Ríos, C., 2012. Lead neurotoxicity: effects on brain nitric oxide synthase. J. Mol. Histol. 43, 553–563.
Okumura, H., Shiba, D., Kubo, T., Yokoyama, T., 2008. P2X7 receptor as sensitive flow sensor for ERK activation in osteoblasts. Biochem. Biophys. Res. Commun. 372, 486–490.
Pal, M., Sachdeva, M., Gupta, N., Mishra, P., Yadav, M., Tiwari, A., 2015. Lead exposure in different organs of mammals and prevention by curcumin-nanocurcumin: a review. Biol. Trace Elem. Res. 168, 380–391.
Rajendra Acharya, U., Paul Joseph, K., Kannathal, N., Lim, C.M., Suri, J.S., 2006. Heart rate variability: a review. Med. Biol. Eng. Comput. 44, 1031–1051.
Rozental, R., Srinivas, M., Spray, D.C., 2001. How to close a gap junction channel. Efficacies and potencies of uncoupling agents. Methods Mol. Biol. 154, 447–476.
Sadek, A.R., Knight, G.E., Burnstock, G., 2011. Electroconvulsive therapy: a novel hypothesis for the involvement of purinergic signalling. Purinergic Signalling 7, 447–452.
Sanchez-Nogueiro, J., Marin-Garcia, P., Bustillo, D., Olivos-Ore, L.A., Miras-Portugal, M.T., Artalejo, A.R., 2014. Subcellular distribution and early signalling events of P2X7 receptors from mouse cerebellar granule neurons. Eur. J. Pharmacol. 744, 190–202.
Sim, J.A., Young, M.T., Sung, H.Y., North, R.A., Surprenant, A., 2004. Reanalysis of P2X7 receptor expression in rodent brain. J. Neurosci. Off. J. Soc. Neurosci. 24, 6307–6314.
Song, H., Zheng, G., Liu, Y., Shen, X.F., Zhao, Z.H., Aschner, M., Luo, W.J., Chen, J.Y., 2016. Cellular uptake of lead in the blood-cerebrospinal fluid barrier: novel roles of Connexin 43 hemichannel and its down-regulations via Erk phosphorylation. Toxicol. Appl. Pharmacol. 297, 1–11.
Sperlagh, B., Vizi, E.S., Wirkner, K., Illes, P., 2006. P2X7 receptors in the nervous system. Prog. Neurobiol. 78, 327–346.
Tsao, D.A., Yu, H.S., Cheng, J.T., Ho, C.K., Chang, H.R., 2000. The change of beta-adrenergic system in lead-induced hypertension. Toxicol. Appl. Pharmacol. 164, 127–133.
Tu, G., Li, G., Peng, H., Hu, J., Liu, J., Kong, F., Liu, S., Gao, Y., Xu, C., Xu, X., Qiu, S., Fan, B., Zhu, Q., Yu, S., Zheng, C., Wu, B., Peng, L., Song, M., Wu, Q., Liang, S., 2013. P2X(7) inhibition in stellate ganglia prevents the increased sympathoexcitatory reflex via sensory-sympathetic coupling induced by myocardial ischemic injury. Brain Res. Bull. 96, 71–85.
Vaziri, N.D., 2008. Mechanisms of lead-induced hypertension and cardiovascular disease. Am. J. Physiol. Heart Circ. Physiol. 295, H454–H465.
Vaziri, N.D., Gonick, H.C., 2008. Cardiovascular effects of lead exposure. Indian J. Med. Res. 128, 426–435.
Verkhratsky, A., Parpura, V., Rodriguez, J.J., 2011. Where the thoughts dwell: the physiology of neuronal-glial “diffuse neural net”. Brain Res. Rev. 66, 133–151.
Warwick, R.A., Hanani, M., 2013. The contribution of satellite glial cells to chemotherapy-induced neuropathic pain. Eur. J. Pain 17, 571–580.
Yu, H., Liao, Y., Li, T., Cui, Y., Wang, G., Zhao, F., Jin, Y., 2016. Alterations of synaptic proteins in the hippocampus of mouse offspring induced by developmental lead exposure. Mol. Neurobiol. 53, 6786–6798.
Zahner, M.R., Li, D.-P., Chen, S.-R., Pan, H.-L., 2003. Cardiac vanilloid receptor 1-expressing afferent nerves and their role in the cardiogenic sympathetic reflex in rats. J. Physiol. 551, 515–523.
Zaidi, Z.F., Matthews, M.R., 2013. Source and origin of nerve fibres immunoreactive for substance P and calcitonin gene-related peptide in the normal and chronically denervated superior cervical sympathetic ganglion of the rat. Auton. Neurosci. 173, 28–38.
Zhang, X.F., Han, P., Faltynek, C.R., Jarvis, M.F., Shieh, C.C., 2005. Functional expression of P2X7 receptors in non-neuronal cells of rat dorsal root ganglia. Brain Res. 1052, 63–70.
Zhang, H., Mei, X., Zhang, P., Ma, C., White, F.A., Donnelly, D.F., Lamotte, R.H., 2009. Altered functional properties of satellite glial cells in compressed spinal ganglia. Glia 57, 1588–1599.
Zhang, J., Yan, C., Wang, S., Hou, Y., Xue, G., Zhang, L., 2014. Chrysophanol attenuates lead exposure-induced injury to hippocampal neurons in neonatal mice. Neural Regen. Res. 9, 924–930.
Zhu, G., Fan, G., Feng, C., Li, Y., Chen, Y., Zhou, F., Du, G., Jiao, H., Liu, Z., Xiao, X., Lin, F., Yan, J., 2013. The effect of lead exposure on brain iron homeostasis and the expression of DMT1/FP1 in the brain in developing and aged rats. Toxicol. Lett. 216, 108–123.
Zou, J., Vetreno, R.P., Crews, F.T., 2012. ATP-P2X7 receptor signaling controls basal and TNFα-stimulated glial cell proliferation. Glia 60, 661–673.